Journal of Polymer Research (2021) 28:187
https://doi.org/10.1007/s10965-021-02546-6

ORIGINAL PAPER

Synthesis, molecular structure and photovoltaic performance for polythiophenes with β-carboxylate side chains

Jiabin Zhang[1,2] · Lingpeng Yan[1,3] · Hongwei Tan[4] · Xiaochen Liu[5] · Yi Lin[5] · Lianping Zhang[1] · Hongyu Wang[2] · Chang-Qi Ma[1]

Received: 8 February 2021 / Accepted: 19 April 2021
© The Polymer Society, Taipei 2021

Abstract

To lower the HOMO energy level of polythiophenes, carboxylate groups were introduced to the β-position of the thiophene unit, by which two polythiophenes with tetrathiophene (poly[5,5″-(bis-3,3″-((2-butyloctyl)-carboxylate)-2,2′:2′,2″-terthiophene)-*alt*-5-thiophene], **P-4T-2COOR**) or pentathiophene (poly[5,5″-(bis-3,3″-((2-butyloctyl)-carboxylate)-2,2′:2′,2″-terthiophene)-*alt*-5,5′-(2,2′-bithiophene)], **P-5T-2COOR**) repeating unit were synthesized. Absorption spectroscopy and cyclic voltammetry measurements revealed that the β-carboxylate substitution red-shifts the maximum absorption wavelength (λ_{max}^{abs}) in solution owing to the electron accepting nature of the carboxylate group. In addition, the introduction of β-carboxylate reduces the HOMO level from -5.09 eV for **P3HT** to -5.34 eV and -5.18 eV for **P-4T-2COOR** and **P-5T-2COOR**, respectively, which is in good agreement with quantum chemisty calculation results. However, the β-carboxylate side chain showed different orientation to that of P3HT, which leads to weaker intermolecular π-π interaction as confirmed by less red-shited absorption in thin solid film and the quantum calculation results. Polymer solar cells using **P-4T-2COOR** and **P-5T-2COOR** as the electron donor, 3,9-bis(2-methylene-(3-(1,1-dicyanomethylene)-indanone))-5,5,11,11-tetrakis(4-hexylphenyl)-dithieno[2,3-*d*:2′,3′-*d*′]-s-indaceno-[1,2-*b*:5,6-*b*′]di-thiophene (ITIC) as the electron acceptor were fabricated and tested. The **P-4T-2COOR** and **P-5T-2COOR** based cells showed high open circuit (V_{OC}) of 0.73–0.99 V, significantly higher than that of **P3HT** based cell (V_{OC} of 0.52 V), which can be ascribed to the lower HOMO energy levels and less condensed molecular packing of these two polymers.

Keywords Polymer solar cells · Polythiophenes derivatives · Carboxylate substitution · Side chain engineering · Energy band-gap engineering

✉ Hongwei Tan
hongwei.tan@bnu.edu.cn

✉ Chang-Qi Ma
cqma2011@sinano.ac.cn

1 Printable Electronics Research Center, Suzhou Institute of Nano-Tech and Nano-Bionics, Chinese Academy of Sciences, 398 Ruoshui Road, SEID, SIP, Suzhou 215123, P. R. China

2 Department of Chemistry, College of Science, Shanghai University, 99 Shangda Road, Shanghai 200444, P. R. China

3 Institute of New Carbon Materials, Taiyuan University of Technology, 79 Yingze Street, Taiyuan 030024, P. R. China

4 College of Chemistry, Beijing Normal University, 19 Xinjiekouwai Street, Beijing 100875, P. R. China

5 Department of Chemistry, Xi'an Jiaotong-Liverpool University, 111 Renai Road, SEID, SIP, Suzhou 215000, P. R. China

Introduction

Solution-processed polymer bulk-heterojunction solar cells have attracted significant attention because of their unique advantages: low cost, lightweight, easy large-scale production, solution processability, and flexibility [1–4]. To date, the highest power conversion efficiency (PCE) for a single-junction solar cell has exceeded 18% [5]. The rapid development mainly results from the development of polymer donors and small molecular acceptors [6–8]. However, these highly efficient donor materials usually have complex molecular structures and require multiple steps preparation, [9–11], which could limit their commercial application [9]. It is therefore of great interest to simplify the molecular structure of polymers and thus ease the synthesis. Polythiophenes (PT), known for their simple molecular structure, easy synthesis, and excellent electronic properties,

Published online: 27 April 2021

[10–12] are the most widely studied conjugated polymers in PSCs. Especially, poly(3-hexylthiophene) (P3HT) has been the most excellent photovoltaic donor material with high crystallinity, good thermal stability, and high hole mobility [13]. The P3HT:$IC_{71}BA$ (indene-C_{71} bis-adduct) cell showed a high PCE of 7%, [10] and has been used in organic tandem solar cells [14]. However, the PCE of P3HT based cells remains lower than 10%. The main limiting factor for the relatively low PCE of P3HT-based cells is the low open-circuit voltage (V_{OC}, typically 0.6 V), [10, 13, 15–17] owing to the relatively high-lying HOMO level. Chemical modification on P3HT to lower the HOMO energy level and improve the open-circuit voltage is of interest in finding high-performance polythiophene derivatives for PSCs.

In 2006, Hou et al. reported that introducing alkylthio group into the conjugated chain can effectively down-shift the HOMO levels in poly(p-phenylenevinylene) derivatives [18]. Inspired by this finding, the same group functionalized P3HT with alkylthio chains to yield P3HST. The V_{OC} of the P3HST:$PC_{61}BM$ reaches a slightly higher value of 0.63 V [19]. In 2009, Hou et al. reported the synthesis of a new PT derivative P3HDTTT, [20] which is based on a terthiophene repeating unit with branched 2-hexyldecyl side chains. Compared to P3HT, P3HDTTT has a lower alkyl chain density and bulky branch chain, ensure P3HDTTT a lower HOMO level and thus a higher V_{OC} (0.82 V) in P3HDTTT:$PC_{61}BM$ cell.

Introducing electron-withdrawing substituents, such as fluorine, [3, 21–24] chlorine, [25] and carboxylate [25–29] into the molecules unit has been proved to be another feasible strategy to lower the HOMO energy level of organic semiconductors. For example, by introducing the electron-withdrawing chlorine atom onto PDCBT, the HOMO energy level of PDCBT-Cl was decreased from -5.20 to -5.34 eV. As a result, the PDCBT-2Cl:ITIC-Th1 cells showed a high V_{OC} of 0.98 V [25]. Russell and co-workers systematically investigated the impact of fluorine atom content on the photovoltaic performance of PBDTTT-EFT, and found that the best PCE of 8.75% was realized from the PBDTTT polymer with the highest fluorine content along with a high V_{OC} of 0.79 V, which is much higher than that (0.72 V) of PBDTTT polymer with no fluorine atom substituents [24]. In addition, carboxylate is another good substituent for the functionalization of conjugated polymers for its electron-withdrawing nature and the possibility of tuning the resulting polymer's solubility. In 2011, Li et al. reported the synthesis and characterization of a polythiophene derivative (PT-C3), which has one ester substitution on every terthiophene repeating unit. The resulting PT-C3 showed a low HOMO level of − 5.10 eV and a consequent V_{OC} of 0.77 V in PT-C3:$PC_{70}BM$ cell [29]. Further increase of the density of electron-withdrawing groups is expected to deeper the HOMO level of the conjugated polymers. With this, polythiophene derivative with one carboxylate substitution for every bithiophene repeating unit, named PDCBT, was designed and synthesized. As expected, the stronger electron-withdrawing effect of alkyl ester groups further decreased the HOMO level to − 5.26 eV [16]. Following a similar structure modification strategy, polythiophenes with carboxylate side chains and vinylene linker (PBT and PTT) were synthesized [27]. Both polymers displayed deep HOMO energy levels owing to the electron-withdrawing carboxylate groups, and high V_{OC} of 0.8 V was achieved for the corresponding polymers:fullerene cells.

Although new conjugated polymers having carboxylate side chains were reported in the literature, [16, 24–27] carboxylate side-chain functionalized polythiophene was rarely reported [16, 26, 27]. Inspired by these works, we designed and synthesized two new polythiophenes having electron-withdrawing carboxylate substitutions on the β-position of thiophene ring with tetrathiophene (poly[5,5′′-(bis-3,3′′-((2-butyloctyl)-carboxylate)-2,2′:2′,2′′-terthiophene)-*alt*-5-thiophene], **P-4T-2COOR**) or pentathiophene (poly[5,5′′-(bis-3,3′′-((2-butyloctyl)-carboxylate)-2,2′:2′,2′′-terthiophene)-*alt*-5,5′-(2,2′-bithiophene)], (**P-5T-2COOR**) repeating unit. Owing to the electron-withdrawing effect of the carboxylate side chain, the HOMO levels of the two polymers were effectively reduced from -5.09 eV for **P3HT** to -5.18 eV and -5.34 eV, respectively. Bulk heterojunction PSCs based on polymer as the electron donor blended with ITIC as the electron acceptor exhibited PCE and V_{OC} of 3.63% and 0.87 V for **P-4T-2COOR** and 3.73% and 0.80 V for **P-5T-2COOR**, which are much higher than that of P3HT:ITIC cell (1.25%, 0.52 V) [30]. The current work provides a feasible method to lower the HOMO energy of polythiophene derivatives that is important for developing high-performance polymers for polymer solar cells.

Experimental section

Materials

All reagents and chemicals were purchased from commercial sources and used without further purification unless specifically stated. The starting material 3-methylthiophene was purchased from J&K China Chemical Ltd. N-Bromosuccinimide (NBS), benzoyl peroxide (BPO), N,N'-dicyclohexylcarbodiimide (DCC), 4-dimethylaminopyridine (DMAP), trifluoroacetic acid (TFA) and Tetrakis(triphenylphosphine) palladium ($Pd(PPh_3)_4$) were purchased from Adamas. Hexamethylenetetramine (HMTA) and Silver nitrate ($AgNO_3$) were purchased from China National Pharmaceutical Group Chemical Reagent Co. Ltd. 2,5-bis(trimethylstannyl)thiophene and 5,5′-bis(triMethylstannyl)-2,2′-bithiophene were purchased from SunaTech Inc. All solvents came from the purification system. ITIC for solar cell fabrication was

purchased from Solarmer (Beijing) Co. Ltd., and used without further purification.

Synthesis

The target polymers were synthesized via a Stille couple reaction of bis-brominated terthiophene (compound 3) with bis-trimethylstannyl mono- and bithiophenes (Scheme 1). Detailed synthesis procedures and the structural characterization of these compounds are describing as following:

Synthesis of 2-butyloctyl-2-bromothiophene-3-carboxylate (1)

To the mixture of 2-bromo-3-thiophenoic acid (0.40 g, 1.9 mmol), N,N'-dicyclohexylcarbodiimide (DCC, 0.46 g, 2.2 mmol), 4-dimethylaminopyridine (DMAP, 85 mg, 0.6 mmol), and 15 mL CH_2Cl_2 in a 50 mL round-bottom flask were added 2-butyloctan-1-ol (0.36 g, 1.9 mmol). After being stirred for 6 h under N_2, the reaction mixture was poured into 30 mL water and then extracted with CH_2Cl_2. The organic phases were dried with sodium sulfate, and the solvent was removed. The product was purified with column chromatography on silica gel using hexane/CH_2Cl_2 (5:1), yielding the pure compound as a colorless oil (0.61 g, 85%).

^{1}H NMR ($CDCl_3$, 400 MHz) δ (ppm): 7.216 (d, 1H, J = 6 Hz), 7.365 (d, 1H, J = 5.6 Hz), 4.201 (d, 2H, J = 5.6 Hz), 1.761 (m, 1H), 1.275 (m, 16H), 0.876 (m, 6H). ^{13}C NMR ($CDCl_3$, 100 MHz) δ (ppm): 162.14, 131.42, 129.47, 125.75, 119.39, 67.64, 37.29, 31.77, 31.32, 31.01, 29.57, 28.91, 26.67, 22.95, 22.61, 14.06, 14.03.

Synthesis of 3T-2COOR (2)

The compound **1** (310 mg, 0.82 mmol) and 2,5-bis(trimethylstannyl)thiophene (140 mg, 0.34 mmol) were mixed in DMF (6 mL). After the solution was flushed with N_2 for 5 min, $Pd(PPh_3)_4$ (714 mg, 0.1 mmol) was added, and the mixture was further flushed with N_2 for 10 min. The reactants were heated to 80 ℃ for 24 h. The mixture was extracted with chloroform several times, and the organic phases were combined. The solvent was removed, and the crude product was purified with flash column chromatography using hexane/CH_2Cl_2 (2:1) as eluent. The pure product was obtained as a green oil (180 mg, 78%).

^{1}H NMR ($CDCl_3$, 400 MHz) δ (ppm): 7.395 (s, 2H), 7.485 (d, 2H, J = 5.2 Hz), 7.206 (d, 2H, J = 5.2 Hz), 4.151

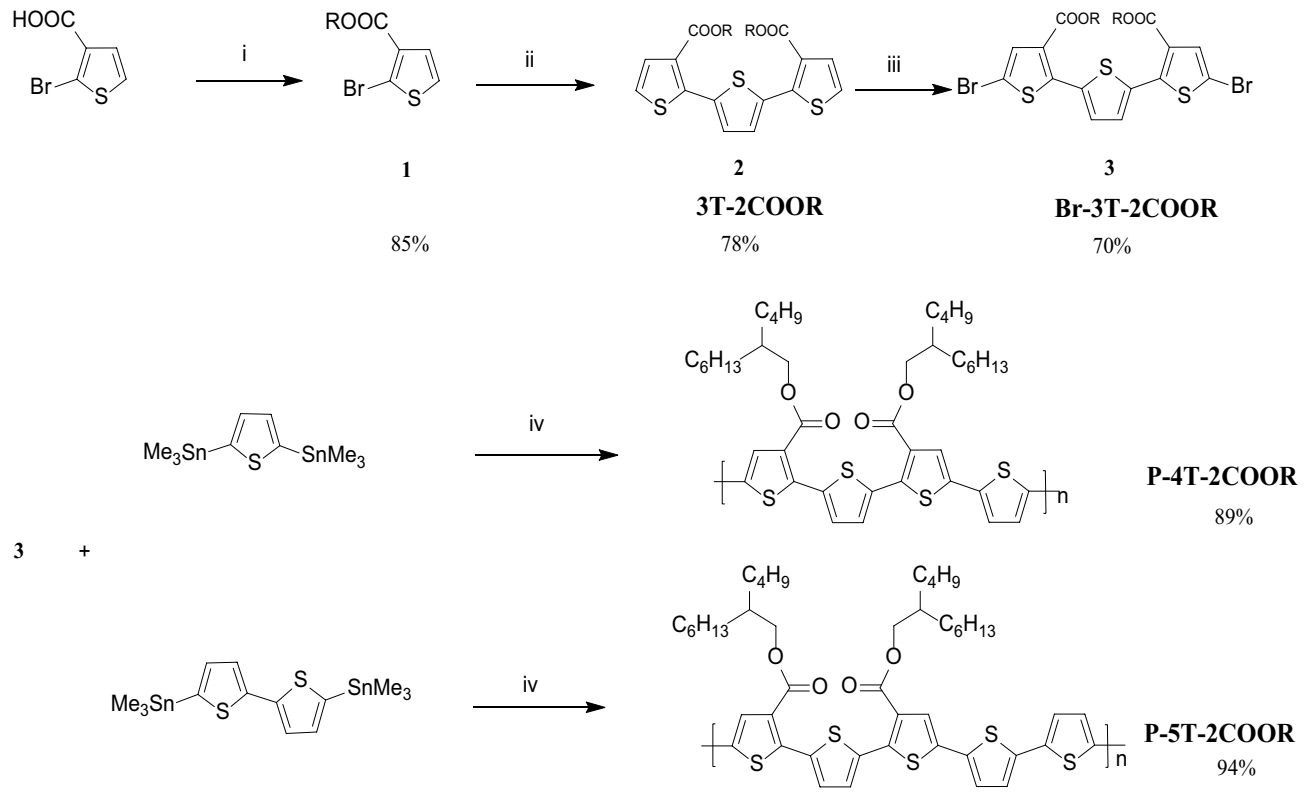

Scheme 1 The synthetic routes for the monmer and polymers. Reagents and conditions: (i) 2-butyloctan-1-ol, DCC, DMAP, CH_2Cl_2, nitrogen, 6 h, room temperature; (ii) 2,5-bis(trimethylstannyl)thiophene, $Pd(PPh_3)_4$, DMF, 24 h, 80 ºC; (iii) NBS, CF_3COOH, DMF, 8 h, room temperature; (iv) $Pd(PPh_3)_4$, toluene, nitrogen, 40 h, 125 ºC.

(d, 4H, $J = 5.6$ Hz), 1.671 (m, 2H), 1.267 (m, 32H), 0.870 (m, 12H). ^{13}C NMR ($CDCl_3$, 100 MHz) δ (ppm): 163.18, 142.44, 135.92, 130.46, 129.09, 128.23, 124.02, 67.57, 37.24, 31.77, 31.25, 30.93, 29.58, 28.87, 26.64, 22.94, 22.60, 14.05, 14.01.

Synthesis of Br-3T-2COOR (3)

Compound **2** (268 mg, 0.4 mmol) was dissolved in DMF (10 mL) and CF_3COOH (1 mL). NBS (170 mg, 0.9 mmol) was then added to the solution, and the resulted solution was stirred for 8 h in the dark. The mixture was then extracted with chloroform several times, and the organic phases were combined. The solvent was removed, and the crude product was purified with flash column chromatography using hexane/CH_2Cl_2 (3:1) as eluent. The pure product was obtained as a green oil (198 mg, 70%).

^{1}H NMR ($CDCl_3$, 400 MHz) δ (ppm): 7.423 (s, 2H), 7.335 (s, 2H), 4.132 (d, 4H, $J = 5.6$ Hz), 1.671 (m, 2H), 1.267 (m, 32H), 0.870 (m, 12H). ^{13}C NMR ($CDCl_3$, 100 MHz) δ (ppm): 161.95, 143.50, 135.27, 132.72, 129.41, 128.54, 111.05, 67.92, 37.22, 31.80, 31.24, 30.92, 29.58, 28.89, 26.65, 22.95, 22.63, 14.09, 14.04.

Synthesis of P-5T-2COOR

The monomer **3** (317 mg, 0.38 mmol) and 2 5,5′-bis(trimethylstannyl)-2,2′-bithiophene (188 mg, 0.38 mmol) were mixed in 20 mL toluene. After the solution was flushed with N_2 for 5 min, $Pd(PPh_3)_4$ (8 mol%) was added, and the mixture was further flushed with N_2 for 10 min. The reactants were heated to 125 ºC for 40 h. After cooling to room temperature, the crude polymer was precipitated by the addition of methanol (100 mL) and then filtered. It was then subjected to Soxhlet extraction with methanol, hexane, and chloroform. The corresponding polymer was recovered as a solid powder from the chloroform fraction by precipitation from methanol. After the polymer was dried under vacuum and the desired product was obtained as a solid with a yield of 94%.

GPC ($CHCl_3$, 45 °C): $M_n = 17.3$ K, $M_w = 77.8$ K, PDI = 4.5.

P-4T-2COOR was synthesized by the same method and got the yield of 89%, GPC ($CHCl_3$, 45 °C): $M_n = 22.4$ K, $M_w = 56.7$ K, PDI = 2.5.

Measurements and characterization

The ^{1}H NMR and ^{13}C NMR spectrum of the synthesized chemical were obtained on Varian MR 400 MHz and on a Brucker Avance III 400 MHz NMR spectrometer. Chemical shifts are reported in δ (ppm), referenced to tetramethylsilane (TMS) as the internal standard. The polymer's molecular weight was measured by gel permeation chromatography (GPC) on a Waters 1515 system equipped with a HR2 (pore size: 500 Å) column and a refractive index detector using chloroform as the mobile phase and monodisperse polystyrene as the external standard. UV–Vis spectra of these new materials in chloroform ($CHCl_3$) solution and thin film were recorded on a Perkin Elmer Lambda 750 UV–Vis Spectrophotometer. For UV–Vis absorption measurement in solution, the concentrated solutions (around 0.08 mg/mL) were prepared independently and then were further diluted to a series of solutions for the measurement. Thin film samples for UV–Vis measurements were prepared by spin-casting a chloroform solution (around 10 mg/mL) on quartz substrates. The thermogravimetric analysis (TGA) of the polymers was performed on Perkin Elmer TGA under N_2 at a heating rate of 10 ºC/min. Cyclic voltammetry (CV) experiments were performed with an Autolab PGSTAT 302G Electrochemistry Workstation. All CV measurements were carried out at room temperature with a conventional three-electrode configuration under N_2. The electrochemical cyclic voltammetry was performed in a 0.1 $mol \cdot L^{-1}$ tetrabutylammonium hexafluorophosphate (Bu_4NPF_6)/acetonitrile solution with a scan speed of 0.05 $V \cdot s^{-1}$. A Pt disk ($\phi = 1$ mm) embedded in Teflon was used as the working electrode. The surface was polished before use. A Pt sheet (~ 1 cm^2) and Ag/AgCl were used as the counter and reference electrodes, respectively. A ferrocene/ferrocenium (Fc/Fc^+) redox couple was used as an external standard. The concentration of the polymer solution was 0.5 mg/mL in chlorobenzene for CV measurement. The solution was then dropped onto the working electrode until a thin film is shaped on the surface of the electrode.

Conformations of polythiophenes in solution were obtained from molecular dynamics simulations. For each of the polythiophene, MD simulation was performed for 60 ps with a step size of 1 fs. Semiempirical molecular orbital method PM6 was employed in the simulations [31]. For the geometric structures of polythiophenes in the film, dimer models were constructed for **P-4T-2COOR** and **P-5T-2COOR**, respectively, which were then submitted to optimization by using PM6 method. CP2K [32] and Gaussian 09 program were employed to perform the MD simulations and geometry optimization, respectively. The X-ray diffraction (XRD) spectrum was recorded by a D8 Advance XRD instrument operated with Cu Kα radiation. Layer thickness of the photoactive layer was measured by a Bruker Dektak 150. Thin solid films for the XRD experiments were deposited on quartz substrates. Atomic force microscopy (AFM) images were acquired with a Dimension ICON in tapping mode.

Fabrication and characterization of OPV cells

ITO-coated glass substrates were cleaned with detergent, de-ionized water, acetone, and isopropyl alcohol in turn by an ultrasonic-wave cleaner, and then dried under a flow of dry nitrogen. Prior to the deposition of the organic layer, the substrates were finally cleaned in UV-ozone for 30 min to eliminate any remaining organic component. For device fabrication, a thin layer of ZnO (ca. 20 nm) was deposited onto pre-cleaned ITO-coated glass by spin-coating a dispersion of ZnO nanoparticles in methanol at 2300 rpm. The substrates were also baked at 120 °C for 10 min in the nitrogen-filled glove box. Subsequently, the active layer (around 85–100 nm) was spin-coated on the ZnO layer using a homogeneous solution of polymers and ITIC. Then, the prepared thin film was dried slowly at 120 °C for 10 min in the nitrogen-filled glove box. The blended mixture of polymers and ITIC were dissolved in chlorobenzene use different volumes with a total concentration of 20 mg·mL^{-1} under different D/A ratio and volume ratio 1,8-diiodooctane (DIO). The solutions were stirred overnight at 75 °C prior to use. At the final stage, MoO_3 (20 nm)/Al (ca. 100 nm) electrode was thermally deposited under a pressure of about 1.0×10^{-4} Pa through a mask on top of the active layer for the inverted devices.

Result and discussion

Synthesis of the polymers

The carboxylate functionalized polythiophenes are mostly based on 3,3′-biscarboxylat-2,2′-bithiohene building blocks, where the two thiophene units having carboxylate side chain are linked directly [16, 25]. To reduce the steric hindrance between two carboxylate groups, the monomer Br-3 T-2COOR was designed as the building block, where one thiophene unit was inserted between two carboxylate chains thiophenes unit. It was synthesized in three steps starting from the 2-bromothiophene-3-carboxylic acid with an overall yield of 46% (Scheme 1). Stille coupling of Br-3 T-2COOR with corresponding stannic mono- and bithiophene derivatives gave two PT derivatives, **P-4T-2COOR** and **P-5T-2COOR**, with excellent yields of 94% and 89%, respectively. Both polymers showed good solubility in common solvents such as chloroform, chlorobenzene and dichlorobenzene. The molecular weights and polydispersity indices (PDIs) were measured by gel permeation chromatography (GPC). The number average molecular weights (M_n) of **P-4T-2COOR** and **P-5T-2COOR** were 22.4 K and 17.3 K with PDI of 2.5 and 4.5, respectively. The results are shown in supporting information (Figure S1). The thermal properties of **P-4T-2COOR** and **P-5T-2COOR** were investigated by thermogravimetric analysis (TGA) under N_2 with a heating rate of 10 ºC/min. The results showed that the decomposition temperatures of **P-4T-2COOR** and **P-5T-2COOR** at 5% weight loss are 356 ºC and 346 ºC, respectively (supporting information, Figure S2), indicating that these two polymers have good thermal stability, which ensured the processing and application of PSCs.

Optical and electrochemical properties

These two polymers' photophysical properties were investigated by UV–Vis absorption spectroscopy in dilute chloroform solution and in film spin-coated on quartz substrates. The UV–Vis absorption spectra of polymers are shown in Fig. 1. Spectroscopic data of polymer and **P3HT** are summarized in Table 1. In solution, **P-4T-2COOR and P-5T-2COOR** showed a broad absorption band with peak absorption wavelength (λ_{abs}^{max}) at 465 nm and 476 nm, which were red-shifted by 15 nm and 26 nm compared to that of P3HT, owing to the electron-accepting nature of the carboxylate groups (vide supra). In the thin-film state, it is common to observe red shifts for the absorption spectra due to the intensive intermolecular interactions when compared to the corresponding solution state [29]. Unlike P3HT, which showed a large red-shift of 105 nm from the solution to the thin solid film for the absorption maxima (λ_{abs}^{max}), both **P-4T-2COOR** and **P-5T-2COOR** showed less pronounced red-shifts of 64 and 53 nm, suggesting that less intensive interaction for these two carboxylate group functionalized polythiophenes in thin solid state. The absorption onset (λ_{abs}^{onset}) of the spectra were measured to be 675, 652 and 668 nm for **P-4T-2COOR**, **P-5T-2COOR** and **P3HT**, respectively corresponding to the E_g^{opt} of 1.84, 1.90 and 1.80 eV, respectively, as calculated from the equation of $E_g^{opt} = 1240/\lambda_{abs}^{onset}$.

Electrochemical cyclic voltammetry (CV) was employed to investigate redox behaviors of conjugated polymers and to determine the HOMO and the lowest unoccupied molecular orbital (LUMO) levels [33]. CV curves were shown in Fig. 1b and the relevant data are summarized in Table 1. The onset oxidation potentials (E_{ox}^{onset}) are 0.54 V versus Fc/Fc$^+$ for **P-4T-2COOR**, 0.38 V for **P-5T-2COOR** and 0.29 V for **P3HT**, respectively. While the onset reduction potentials (E_{red}^{onset}) are -1.87, -1.85 and -2.27 V, respectively. It worth pointing out that the CV curves of these polymers are different to each other, which could be ascribed to the difference of polymer layer thickness, since the thin films for CV measurement were prepared by drop casting the solution onto the Pt electrode directly.

From the E_{ox}^{onset} and E_{red}^{onset} of polymers, HOMO and LUMO levels were determined according to the equations [34].

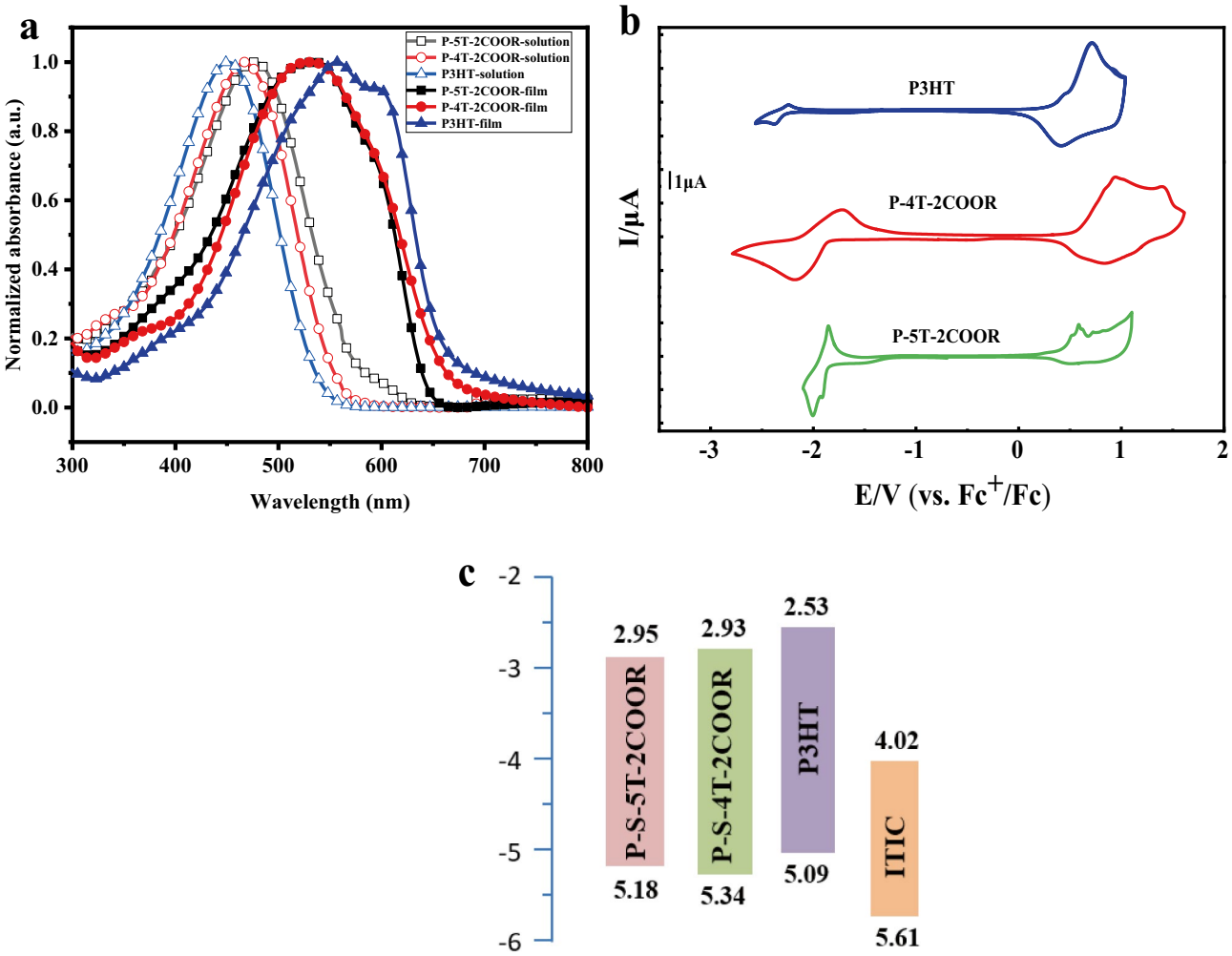

Fig. 1 (**a**) Normalized UV–Vis absorption spectra of **P-4T-2COOR**, **P-5T-2COOR** and **P3HT** in solution and film; (**b**) Cyclic voltammetry curve of the polymer films coated on a platinum electrode, measured in 0.1 mol/L Bu_4NPF_6 acetonitrile solutions at a scan rate of 100 mV/s; (**c**) Energy level diagrams of **P-4T-2COOR**, **P-5T-2COOR**, **P3HT** and ITIC

E_{HOMO} = -e (E_{ox}^{onset} + 4.8) (eV) E_{LUMO} = -e (E_{red}^{onset} + 4.8) (eV).

From Table 1, it can be seen that both LUMO energy and HOMO energy levels are lower than those of **P3HT**. The decrease of HOMO energy level was mainly due to the introduction of electron-withdrawing carboxylate substitutions in side chain of polymers. This was very beneficial for achieving higher V_{OC} in PSCs. In fact HOMO energy level significantly decreased from -5.09 eV for **P3HT** to -5.34 eV and -5.18 eV for **P-4T-2COOR** and **P-5T-2COOR**, respectively.

Molecular conformation and packing behaviors

To better understand the influence of the β-carboxylate groups on the electronic structures and molecular confirmation of the polymers, quantum chemical calculations was performed on these two compounds. For comparison, the quantum chemical calculation was also performed on P3HT. Figure 2 showed the optimized molecular geometries and frontier molecular orbitals of these three polythiophenes. For P3HT, all the thiophene units are linked in an *anti*-conformation and the alkyl side chains are pointing towards outside the conjugation chain, similar to that reported in the literature [35]. For **P-4T-2COOR** and **P-5T-2COOR**, the closest two β-carboxylate groups, are on the 3,3′′-position of terthiophene unit (**3T-2COOR** in Scheme 1), which has much less steric hindrance than that on the 3,3′-position of bithiophene as usually found in regio-random P3HT. Therefore, the β-carboxylate substituents of the polythiophene do not influence the structural conformation of the conjugation skeleton, and all thiophene units are linked via an anti-confirmation as well for **P-4T-2COOR** and **P-5T-2COOR** (Fig. 2). The

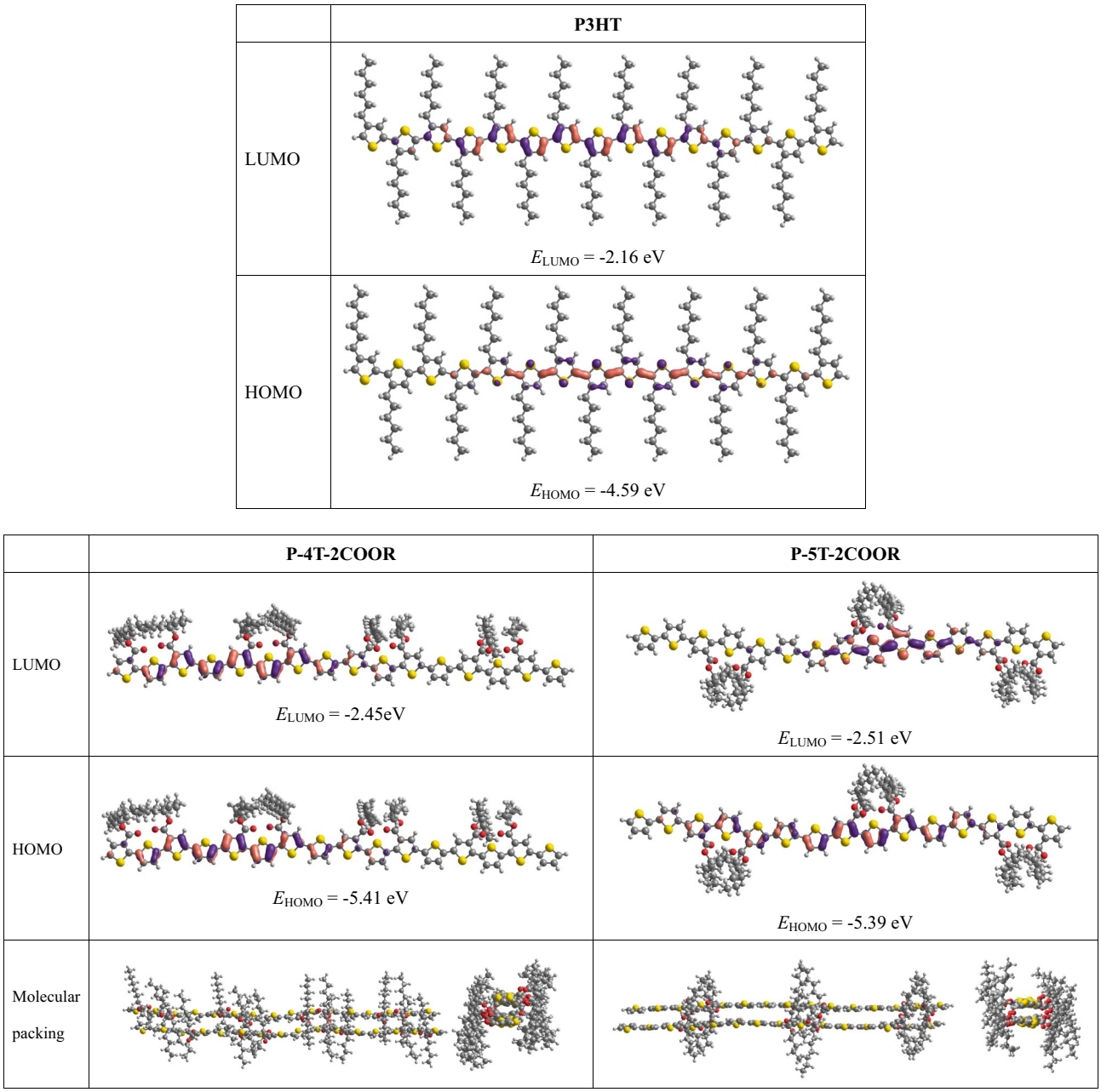

Fig. 2 Optimized molecular geometrys, molecular orbitals and molecular packing of **P-4T-2COOR** and **P-5T-2COOR**. Molecular structure and orbitals of P3HT are also listed for comparaion

calculated electron cloud of the HOMO orbitals of these polythiophenes are found to be mainly delocalized over 7–8 thiophene units with energy levels of -4.59, -5.41, and -5.39 eV for P3HT, **P-4T-2COOR** and **P-5T-2COOR**, respectively. Clearly, the introduction of β-carboxylate side chain significantly reduces the HOMO energy level of the final polythiophene. The carboxylate group is directly involved in the LUMO orbital through conjugating to the polythiophene chain, and the LUMO energy levels of **P-4T-2COOR** and **P-5T-2COOR** are calculated to be -2.45 and -2.51 eV, respectively, which is also lower than that of P3HT (-2.16 eV).

It is well known that lamellar structure formed within the P3HT molecules, which leads to the formation of crystalline domains in thin solid film [35]. However, owing to the C = O unit of the ester group, the two β-carboxylate groups are found to be perpendicular to the conjugated polythiophene plane in **P-4T-2COOR** and **P-5T-2COOR** (Fig. 2). Although π-π stacking can still be simulated with quantum chemistry calculation, such branched side chains blocks the

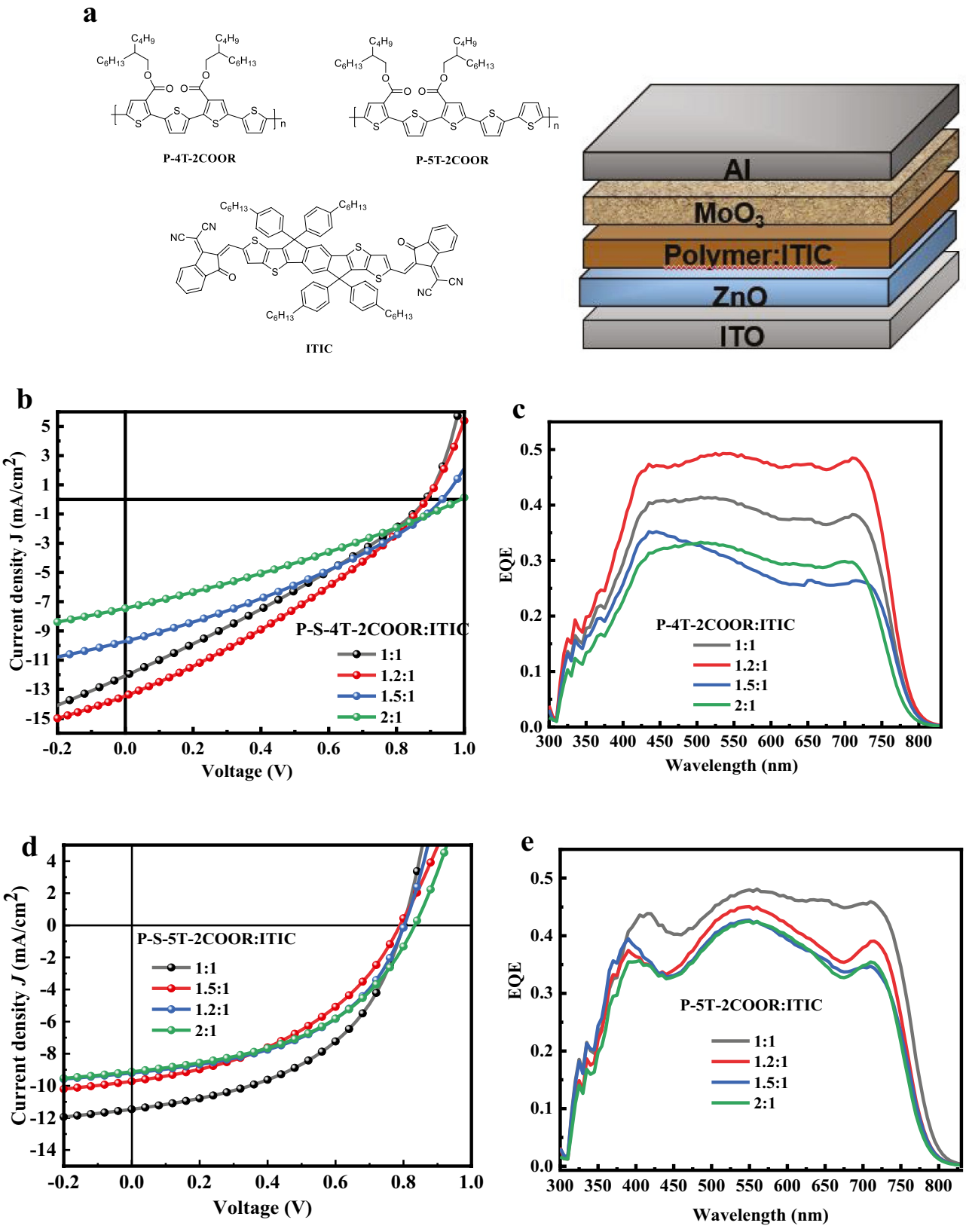

Fig. 3 (**a**) molecular structures and device structure of the polymer solar cells; *J*-*V* curves (**b**, **d**) and EQE (**c**, **e**) based on **P-4T-2COOR**:ITIC (**b**, **c**) and **P-5T-2COOR**:ITIC (**d**, **e**) with different ratios

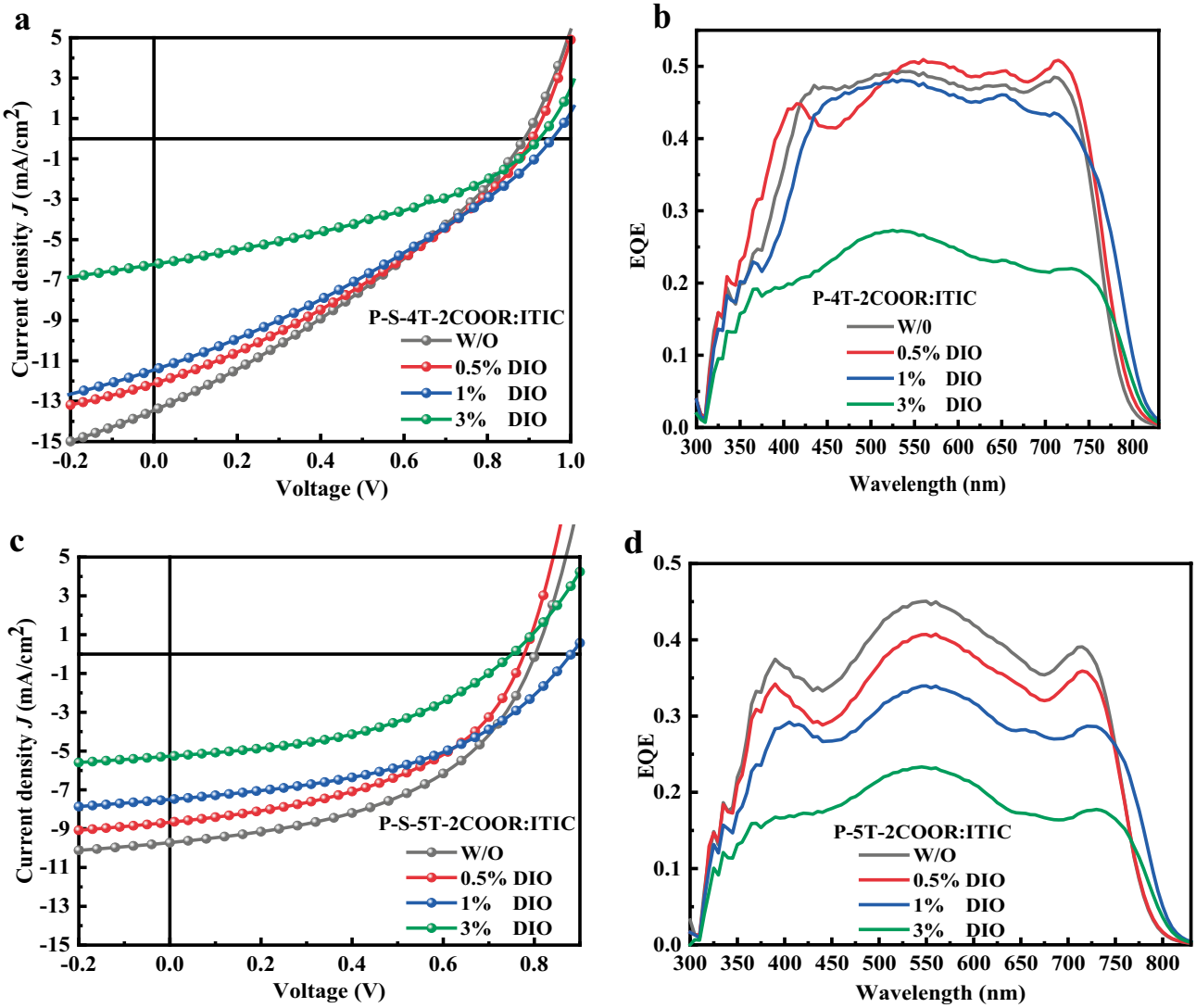

Fig. 4 *J-V* curves (**a**, **b**) and EQE (**c**,**d**) based on **P-4T-2COOR**:ITIC (**a**, **b**) and **P-5T-2COOR**:ITIC (**c**, **d**) with different DIO blending concentrations

intermolecular approaching leading to weak intermolecular interaction in thin solid films. Such a molecular stacking structure explains the relatively small red-shifts of absorption spectra for **P-4T-2COOR** and **P-5T-2COOR** from solution to thin solid film (Fig. 1 and Table 1).

Photovoltaic properties

To investigate and compare the photovoltaic properties of the two polymers, we fabricated and tested the bulk heterojunction PSCs with a structure of ITO/ZnO/polymer:ITIC/MoO_3/Al (Fig. 3a), where the synthesized polymers were used as the electron donor and ITIC [30, 36, 37] was used as the electron acceptor, and the ZnO and MoO_3 were used as the electron and hole transporting layers, respectively. Figure 3b-e showed the *I-V* curves of devices with different D/A weight ratios, and Table 2 lists the corresponding open-circuit voltage (V_{OC}), short-circuit current (J_{SC}), fill factor (FF), and power conversion efficiency (PCE) under simulated AM 1.5G sunlight illumination. In both cases, the optimized D/A ratio was found to be 1.2:1, which leads to the best PCE of 3.63% and 3.73% for **P-4T-2COOR** and **P-5T-2COOR**, respectively, which is much higher than that of P3HT:ITIC cell (1.25%) [30]. More importantly, both devices exhibited higher open-circuit voltage (0.87 V for **P-4T-2COOR**, 0.80 V for **P-5 T-2COOR**), which can be ascribed to the deep HOMO energy level of the two polymers. As shown in Fig. 3, the external quantum efficiency (EQE) of different weight ratios exhibited a broad range from 450 to 750 nm. The maximum EQE value of

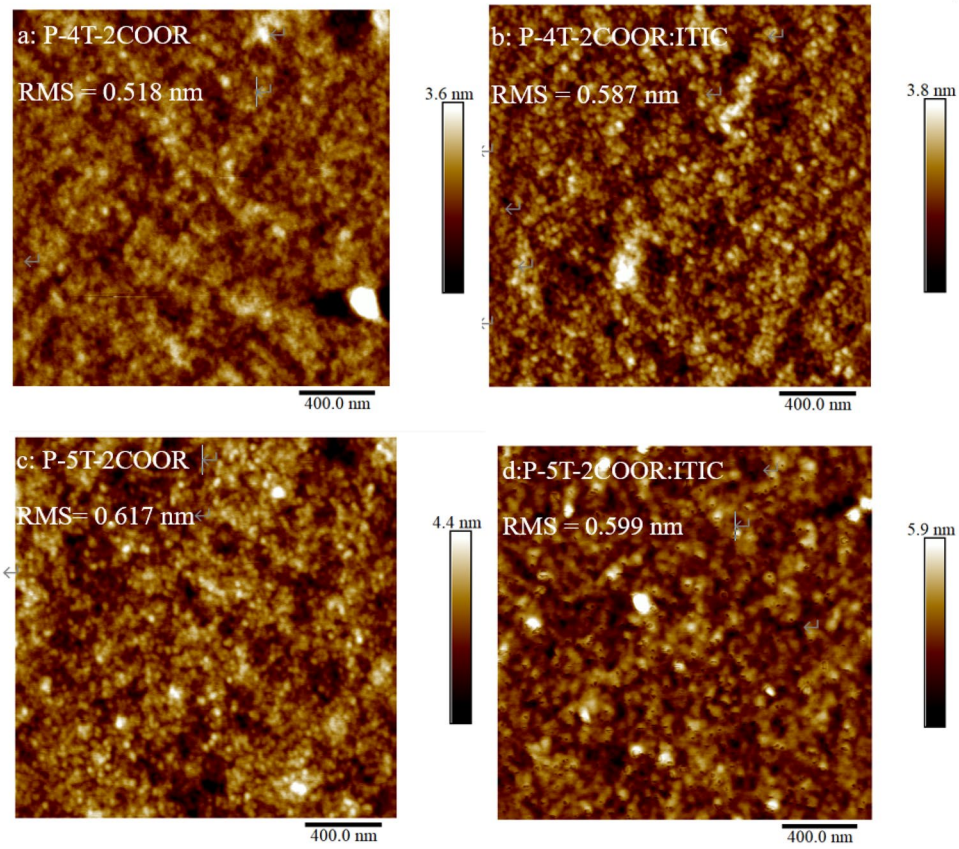

Fig. 5 AFM topology images of the pristine **P-4T-2COOR** and **P-5T-2COOR** (**a**, **c**) and the blended films (**b**, **d**)

device based on **P-4T-2COOR** and **P-5T-2COOR** reached 50% and 45%, respectively and its corresponding J_{SC} were 13.45 mA/cm [2] and 9.71 mA/cm [2]. The **P-4T-2COOR** and **P-5T-2COOR** based cells showed higher V_{OC} and J_{SC} when compared to that of P3HT:ITIC cell, [31]; however, lower FF was found for these two cells when compared to the P3HT cell. This was supposed to be due to the unblanced charge carrier mobility of the **P-4T-2COOR** and **P-5T-2COOR** blend films originated from the unfavorable nano-morphology, since FF is directly related to the charge transport within the blend film [38].

To check whether solvent additive is able to tune the morphology and improve device performance or not, we study the effect of solvent additive (DIO, with D:A 1.2:1 in mass) on devie performance [39, 40]. The *I-V* curves of devices were shown in Fig. 4, and the corresponding data were summarized in Table 3. For **P-5T-2COOR**, with the increase of additive concentration, the J_{SC} decreased, resulting in poorer performance. While for **P-4T-2COOR**, there is a slight increase of performance with the addition of DIO up to 1%, mainly due to the increase of V_{OC}. Further increase of the additive reverse the effect to give poorer performance, as the

Table 1 Optical and electrochemical property parameters of **P-5T-2COOR**, **P-4T-2COOR** and **P3HT**

Polymers	λ_{abs}^{max} (nm)[a]	λ_{film}^{max} (nm)[b]	λ_{abs}^{onset} (nm)[b]	E_g^{opt} (eV)[c]	E_{ox}^{on} (V)[d]	E_{red}^{on} (V)[d]	E_{HOMO} (eV)[e]	E_{LUMO} (eV)[e]	E_g^{cv} (eV)[f]
P-4T-2COOR	465	529	675	1.84	0.54	-1.87	-5.34	-2.93	2.41
P-5T-2COOR	476	529	652	1.90	0.38	-1.85	-5.18	-2.95	2.23
P3HT	450	555, 600	668	1.85	0.29	-2.27	-5.09	-2.53	2.56

[a]In $CHCl_3$ solution (0.08 mg/mL)

[b]Spin-coated from $CHCl_3$ solution (10 mg/mL) onto the quartz

[c]Calculated from the absorption edge of polymer film $E_g^{opt} = 1240/\lambda_{onset}$

[d]Onset oxidation (Eox) and reduction (Ered) potentials of the polymers

[e]HOMO = -e (E_{ox}^{onset} + 4.8) (eV); LUMO = -e (E_{red}^{onset} + 4.8) (eV)

[f]$E_g^{cv} = e(E_{ox}^{onset} - E_{red}^{onset})$

Table 2 Photovoltaic properties of the PSCs based on polymers:ITIC with different weight ratios under the illumination of 100 mW/cm^2

Polymers	D:A (w/w)	V_{OC} (V)	J_{SC}[b](mA/cm^2)	FF	Best PCE	Aver. PCE[c] (±std.dev.)
P-4T-2COOR	1:1	0.94	9.71	0.31	2.83	2.56(±0.19)
	1.2:1	0.87	13.45	0.31	3.63	3.31(±0.31)
	1.5:1	0.88	12.04	0.30	3.18	2.59(±0.60)
	2:1	0.99	7.45	0.29	2.14	2.01(±0.15)
P-5T-2COOR	1:1	0.73	11.46	0.38	3.18	3.05(±0.11)
	1.2:1	0.80	9.71	0.48	3.73	3.66(±0.05)
	1.5:1	0.79	9.19	0.42	3.05	2.99(±0.04)
	2:1	0.84	9.12	0.45	3.45	3.29(±0.12)
P3HT[d]	1:1	0.52	4.22	0.56	1.25	
PDCBT[e]	1:1	0.91	11.0	0.72	7.20	

[a]: weight ratio

[b]: Calculated by convoluting the spectral response with the AM 1.5G spectrum

[c]: The average values were obtained from over 8 devices

[d]: device with a structure of ITO/PEDOT:PSS/active layer/PFN-Br/Al, data cited from reference [30]

[e]. device with a structure of ITO/PEDOT:PSS/PDCBT:$PC_{71}BM$/Ca/Al, data cited from reference [16]

decrease of the J_{SC} offsets the benefit of the increased V_{OC}. These results indicate that the introduction of β-carboxylate side chain on the polythiophene chain changes the intermolecular interaction, leading to different morphology control for solar cell performance optimization.

To understand the correlation between the molecular structure and device performance, the surface morphology and the crystallinity of the pristine polymer and the polymer:ITIC blend films were characterized with AFM. Figures 5a-d show the topology images of **P-4T-2COOR** and **P-5T-2COOR** films with or without blending with ITIC. As seen here, all these films are smooth with low RMS of 0.52–0.62 nm. No obvious nanostructure was observed for the pristine polymer films, suggesting that both **P-4T-2COOR** and **P-5T-2COOR** are not crystalline materials, which could be ascribed to the bulky carboxylate side chains (vide supra). Also these **P-4T-2COOR**:ITIC and **P-5T-2COOR**:ITIC films showed very smooth surface morphology, indicating that ITIC is well intermixed with **P-4T-2COOR** and **P-5T-2COOR**. The absence of nanocrystalline within the photoactive layer is then ascribed to the low device performance in PSCs. Replacing the branched carboxylate chain could be an option to reduce the steric hindrance between polymers and consequently improve the polymer's crystalline property could be able to improve the photovoltaic performance of the carboxylate based polythiophene donors for use in polymer:nonfullenere acceptor solar cells.

Table 3 Photovoltaic properties of the PSCs based on polymers:ITIC with different DIO blending concentrations under the illumination of 100 mW/cm [2].

Devices[a]	DIO (*vol %*)[b]	V_{OC} (V)	J_{SC}[c] (mA/cm^2)	FF	Best PCE	Aver. PCE[d] (±std.dev.)
P-4T-2COOR:ITIC	0	0.87	13.45	0.31	3.63	3.31(±0.31)
	0.5	0.91	12.12	0.32	3.53	3.37(±0.18)
	1.0	0.96	11.45	0.31	3.41	3.38(±0.03)
	3.0	0.92	6.22	0.37	2.12	2.03(±0.07)
P-5T-2COOR:ITIC	0	0.80	9.71	0.48	3.73	3.66(±0.05)
	0.5	0.78	8.67	0.47	3.18	2.89(±0.45)
	1.0	0.88	7.49	0.47	3.10	3.02(±0.07)
	3.0	0.72	5.26	0.43	1.63	1.43(±0.21)

[a]All devices was under D:A ratio of 1.2:1 (w:w)

[b]volume ratio of DIO to the overall volume of solvent

[c]Calculated by convoluting the spectral response with the AM 1.5G spectrum

[d]The average values are obtained from over 8 devices

Conclusion

In summary, two polythiophene derivatives **P-4T-2COOR** and **P-5T-2COOR** with carboxylate side chains, were synthesized and characterized. Compared to **P3HT**, the introduction of electron-withdrawing carboxylate groups of polymers significantly decreased the HOMO energy level. The polymer solar cell of the two polymers blended with ITIC as acceptor exhibited relatively high open-circuit voltage of 0.80 V and 0.88 V, respectively. The PSCs based on **P-4T-2COOR**:ITIC showed PCE of 3.63% with V_{OC} of 0.88 V, J_{SC} of 13.45 mA/cm^2 and FF of 0.32, while that based on **P-5T-2COOR**:ITIC exhibited optimal PCE of 3.73% with V_{OC} of 0.80 V, J_{SC} of 9.71 mA/cm^2 and FF of 0.48. The work suggested that incorporating electron-withdrawing substituents within the molecular structure will be an effective strategy for adjusting the molecular orbital energy levels. Further reduce the steric hindrance of the carboxylate side chains is suggested to increase the crystalline property of the polymers, which should further improve device efficiency.

Supplementary information The online version contains supplementary material available at https://doi.org/10.1007/s10965-021-02546-6.

Acknowledgments This work was supported by Xi'an Jiaotong-Liverpool University Research Development Fund (RDF-14-02-46), and the National Natural Science Foundation of China (22075315).

Declarations

Conflict of interest There is no conflict of interest involved in the work.

References:

1. Wang M, Hu X, Liu P, Li W, Gong X, Huang F, Cao Y (2011) Donor-acceptor conjugated polymer based on naphtho [1,2-c:5,6-c] bis [1,2,5] thiadiazole for high-performance polymer solar cells. J. Am. Chem. Soc. 133:9638–9641
2. Li Y, Zou Y (2008) Conjugated Polymer Photovoltaic Materials with Broad Absorption Band and High Charge Carrier Mobility. Adv. Mater. 20:2952–2958
3. Stuart AC, Tumbleston JR, Zhou H, Li W, Liu S, Ade H, You W (2013) Fluorine substituents reduce charge recombination and drive structure and morphology development in polymer solar cells. J. Am. Chem. Soc. 135:1806–1815
4. Lu L, Zheng T, Wu Q, Schneider AM, Zhao D, Yu L (2015) Recent Advances in Bulk Heterojunction Polymer Solar Cells. Chem. Rev. 115:12666–12731
5. Liu Q, Jiang Y, Jin K, Qin J, Xu J, Li W, Xiong J, Liu J, Xiao Z, Sun K, Yang S, Zhang X, Ding L (2020) 18% Efficiency organic solar cells. Sci.. Bull. 65:272–275
6. Li G, Li W, Guo X, Guo B, Su W, Xu Z, Zhang M (2019) A new narrow bandgap polymer as donor material for high performance non-fullerene polymer solar cells. Org. Electron. 64:241–246
7. Kim H, Lee H, Seo D, Jeong Y, Cho K, Lee J, Lee Y (2015) Regioregular Low Bandgap Polymer with Controlled Thieno[3,4-b]thiophene Orientation for High-Efficiency Polymer Solar Cells. Chem. Mater. 27:3102–3107
8. Lee J, Sin DH, Moon B, Shin J, Kim HG, Kim M, Cho K (2017) Highly crystalline low-bandgap polymer nanowires towards high-performance thick-film organic solar cells exceeding 10% power conversion efficiency. Energy Environ. Sci. 10:247–257
9. Li N, McCulloch I, Brabec CJ (2018) Analyzing the efficiency, stability and cost potential for fullerene-free organic photovoltaics in one figure of merit. Energy Environ. Sci. 11:1355–1361
10. Guo X, Cui C, Zhang M, Huo L, Huang Y, Hou J, Li Y (2012) High efficiency polymer solar cells based on poly(3-hexylthiophene)/indene-C70 bisadduct with solvent additive. Energy Environ. Sci. 5:7943–7949
11. Qian D, Ma W, Li Z, Guo X, Zhang S, Ye L, Ade H, Tan Z, Hou J (2013) Molecular design toward efficient polymer solar cells with high polymer content. J. Am. Chem. Soc 135:8464–8467
12. Fan Q, Su W, Guo X, Guo B, Li W, Zhang Y, Wang K, Zhang M, Li Y (2016) A new polythiophene derivative for high efficiency polymer solar cells with PCE over 9%. Adv. Energy Mater. 6
13. Dang MT, Hirsch L, Wantz G (2011) P3HT:PCBM, best seller in polymer photovoltaic research. Adv. Mater. 23:3597–3602
14. Khlyabich PP, Burkhart B, Thompson BC (2011) Efficient ternary blend bulk heterojunction solar cells with tunable open-circuit voltage. J. Am. Chem. Soc. 133:14534–14537
15. Dennler G, Scharber MC, Brabec CJ (2009) Polymer-fullerene bulk-heterojunction solar cells. Adv. Mater. 21:1323–1338
16. Zhang M, Guo X, Ma W, Ade H, Hou J (2014) A polythiophene derivative with superior properties for practical application in polymer solar cells. Adv. Mater. 26:5880–5885
17. Zhang H, Ye L, Hou J (2015) Molecular design strategies for voltage modulation in highly efficient polymer solar cells. Poly. Intern. 64:957–962
18. Hou J, Fan B, Huo L, He C, Yang C, Li Y (2006) Poly(alkylthio-p-phenylenevinylene): Synthesis and electroluminescent and photovoltaic properties. J. Poly. Sci. A. Polym. Chem. 44:1279–1290
19. Huo L, Zhou Y, Li Y (2009) Alkylthio-substituted polythiophene: absorption and photovoltaic properties. Macromol. Rapid. Commun. 30:925–931
20. Hou J, Chen TL, Zhang S, Huo L, Sista S, Yang Y (2009) An easy and effective method to modulate molecular energy level of Poly(3-alkylthiophene) for high-voc polymer solar cells. Macromolecules 42:9217–9219
21. Kranthiraja K, Long DX, Sree VG, Cho W, Cho Y-R, Zaheer A, Lee J-C, Noh Y-Y, Jin S-H (2018) Sequential fluorination on napthaleneamide-based conjugated polymers and their impact on charge transport properties. Macromolecules 51:5530–5536
22. Price SC, Stuart AC, Yang L, Zhou H, You W (2011) Fluorine substituted conjugated polymer of medium band gap yields 7% efficiency in polymer−fullerene solar cells. J. Am. Chem. Soc. 133:4625–4631
23. Peng Q, Liu X, Su D, Fu G, Xu J, Dai L (2011) Novel Benzo[1,2-b:4,5-b′]dithiophene-Benzothiadiazole derivatives with variable side chains for high-performance solar cells. Adv. Mater. 23:4554–4558
24. Liu P, Zhang K, Liu F, Jin Y, Liu S, Russell TP, Yip H-L, Huang F, Cao Y (2014) Effect of fluorine content in Thienothiophene-Benzodithiophene copolymers on the morphology and performance of polymer solar cells. Chem. Mater. 26:3009–3017
25. Wang Q, Li M, Zhang X, Qin Y, Wang J, Zhang J, Hou J, Janssen RAJ, Geng Y (2019) Carboxylate-Substituted Polythiophenes for Efficient Fullerene-Free Polymer Solar Cells: The Effect of Chlorination on Their Properties. Macromolecules 52:4464–4474

26. Park CG, Park GE, Lee JH, Kim A, Kim YU, Park SY, Park SH, Cho MJ, Choi DH (2018) Regioisomeric π-conjugated terpolymers bearing carboxylate substituted thienothiophenyl quarterthiophene and their application to fullerene-free polymer solar cells. Polymer 146:142–150
27. Wang Q, Dong X, He M, Li M, Tian H, Liu J, Geng Y (2018) Polythiophenes with carboxylate side chains and vinylene linkers in main chain for polymer solar cells. Polymer 140:89–95
28. Chen J, Wang L, Yang J, Yang K, Uddin MA, Tang Y, Zhou X, Liao Q, Yu J, Liu B, Woo HY, Guo X (2018) Backbone Conformation Tuning of Carboxylate-Functionalized Wide Band Gap Polymers for Efficient Non-Fullerene Organic Solar Cells. Macromolecules 52:341–353
29. Zhang M, Guo X, Yang Y, Zhang J, Zhang Z-G, Li Y (2011) Downwards tuning the HOMO level of polythiophene by carboxylate substitution for high open-circuit-voltage polymer solar cells. Polym Chem 2:2900–2906
30. Qin Y, Uddin MA, Chen Y, Jang B, Zhao K, Zheng Z, Yu R, Shin TJ, Woo HY, Hou J (2016) Highly Efficient Fullerene-Free Polymer Solar Cells Fabricated with Polythiophene Derivative. Adv. Mater 28:9416–9422
31. Stewart JJ (2007) Optimization of parameters for semiempirical methods V: modification of NDDO approximations and application to 70 elements. J. Mol. Model 13:1173–1213
32. Garcia A, Papior N, Akhtar A, Artacho E, Blum V, Bosoni E, Brandimarte P, Brandbyge M, Cerda JI, Corsetti F, Cuadrado R, Dikan V, Ferrer J, Gale J, Garcia-Fernandez P, Garcia-Suarez VM, Garcia S, Huhs G, Illera S, Korytar R, Koval P, Lebedeva I, Lin L, Lopez-Tarifa P, Mayo SG, Mohr S, Ordejon P, Postnikov A, Pouillon Y, Pruneda M, Robles R, Sanchez-Portal D, Soler JM, Ullah R, Yu VW, Junquera J (2020) Siesta: Recent developments and applications. J. Chem. Phys. 152:204108
33. Li Y, Cao Y, Gao J, Wang D, Yu G, Heeger A (2017) Electrochemical properties of luminescent polymers and polymer light-emitting electrochemical cells. Synth. Met. 99:243–248
34. Cardona CM, Mccarley TD, Kaifer AE (2000) Synthesis, electrochemistry, and interactions with β-cyclodextrin of dendrimers containing a single ferrocene subunit located "off-center". J. Org. Chem. 65:1857–1864
35. McCullough RD, Tristram-Nagle S, Williams SP, Lowe RD, Jayaraman M (1993) Self-orienting head-to-tail poly(3-alkylthiopbenes): New insights on structure-property relationships in conducting polymers. J. Am. Chem. Soc. 115:4910–4911
36. Eastham ND, Logsdon JL, Manley EF, Aldrich TJ, Leonardi MJ, Wang G, Powers-Riggs NE, Young RM, Chen LX, Wasielewski MR, Melkonyan FS, Chang RPH, Marks TJ (2018) Hole-Transfer Dependence on Blend Morphology and Energy Level Alignment in Polymer: ITIC Photovoltaic Materials. Adv. Mater. 30:1704263
37. Liang Q, Han J, Song C, Yu X, Smilgies D-M, Zhao K, Liu J, Han Y (2018) Reducing the confinement of PBDB-T to ITIC to improve the crystallinity of PBDB-T/ITIC blends. J. Mater. Chem. A 6:15610–15620
38. Bartesaghi D, Perez IDC, Kniepert J, Roland S, Turbiez M, Neher D, Koster LJA (2015) Competition between recombination and extraction of free charges determines the fill factor of organic solar cells. Nat. Commun. 6:7083
39. Liang Y, Xu Z, Xia J, Tsai ST, Wu Y, Li G, Ray C, Yu L (2010) For the Bright Future - Bulk Heterojunction Polymer Solar Cells with Power Conversion Efficiency of 7.4%. Adv. Mater. 22:E135-E138
40. Ren G, Ahmed E, Jenekhe SA (2011) Non-Fullerene Acceptor-Based Bulk Heterojunction Polymer Solar Cells: Engineering the Nanomorphology via Processing Additives. Adv. Energy Mater. 1:946–953

Publisher's Note Springer Nature remains neutral with regard to jurisdictional claims in published maps and institutional affiliations.